J Therm Anal Calorim (2010) 101:849–857
DOI 10.1007/s10973-010-0834-5

Transitions/relaxations in polyester adhesive/PET system

Elodie Carsalade · Alain Bernès · Colette Lacabanne · Sophie Perraud · Michel Lafourcade · Michel Savignac

Received: 12 June 2009 / Accepted: 22 April 2010 / Published online: 14 May 2010

Abstract The correlations between the transitions and the dielectric relaxation processes of the oriented poly(ethylene terephthalate) (PET) pre-impregnated of the polyester thermoplastic adhesive have been investigated by differential scanning calorimetry (DSC) and dynamic dielectric spectroscopy (DDS). The thermoplastic polyester adhesive and the oriented PET films have been studied as reference samples. This study evidences that the adhesive chain segments is responsible for the physical structure evolution in the PET-oriented film. The transitions and dielectric relaxation modes' evolutions in the glass transition region appear characteristic of the interphase between adhesive and PET film, which is discussed in terms of molecular mobility. The storage at room temperature of the adhesive tape involves the heterogeneity of the physical structure, characterized by glass transition dissociation. Thus, the correlation between the transitions and the dielectric relaxation processes evidences a segregation of the amorphous phases. Therefore, the physical structure and the properties of the material have been linked to the chemical characteristics.

Keywords Differential scanning calorimetry · Dynamic dielectric spectroscopy · Glass transition · Molecular mobility · Poly(ethylene terephthalate) · Polyester adhesive

E. Carsalade · A. Bernès (✉) · C. Lacabanne
Laboratoire de Physique des Polymères, Université de Toulouse, CIRIMAT Institut Carnot, UMR CNRS 5085, 31062 Toulouse Cedex 09, France
e-mail: bernes@cict.fr

E. Carsalade · S. Perraud
CNES, 31401 Toulouse Cedex 09, France

M. Lafourcade · M. Savignac
Zodiac, Ayguesvives, France

Introduction

The peculiar physical–chemical properties of poly(ethylene terephthalate) (PET) are the subjects of extensive investigation for applications in various fields. The adhesion on PET is also an important subject in the industrial applications. Our study is focused on the thermal behavior of an oriented PET film pre-impregnated with a polyester thermoplastic adhesive, denoted as PET adhesive tape. This polyester adhesive is used to join the PET films which constitute the pressurized envelope of the stratospheric balloons. These balloons are the only vehicles which can stay aloft in the stratosphere that extends through an altitude ranging between 12 and 45 km. This environment imposes a drastic schedule of conditions such as a good behavior in the bonding of oriented PET films up to a temperature of −90 °C. Under these severe thermal conditions, a better comprehension of the role of the interphases in producing a joint with high shear strength is required.

This polyester thermoplastic adhesive is also called the hot melt adhesive since it is melted to become a fluid, so that it can be applied to the polymers to be joined, and then it rehardens when cooled. It is possible that between these two polymers a bond is formed by the diffusion of the polymer molecules on one surface into the molecular network of the other surface [1–3]. Thus, this phenomenon of diffusion gives rise to the formation of an interphase region. This interphase region is of a substantial thickness which is responsible for the specific physical and mechanical properties. These properties are different from those obtained in the bulk of each polymer [4, 5].

Nevertheless, the characterization of the influence of the adhesive chain segments on the macromolecular structure of the PET film remains an unsolved problem.

The aim of this study is to enhance our knowledge of the thermal behavior and the molecular mobility evolution occurring in the oriented PET film, pre-impregnated with the polyester thermoplastic adhesive. Among the various methods of investigation available, the dielectric spectroscopy is used as a powerful tool to characterize the structural reorganization in polymers. It constitutes an alternative choice with regard to the conventional techniques to study an interphase, because the relaxation dipolar entities are sensitive to the local environment even when there exist very similar chemical characteristics between the PET and the polyester adhesive. Therefore, the transition and relaxation processes in PET adhesive tape have been studied by differential scanning calorimetry (DSC) and the dynamic dielectric spectroscopy (DDS), respectively. The oriented PET film and the polyester thermoplastic adhesive have been chosen as references samples.

Materials and methods

Materials

A series of PET films were used in this study. The biaxially oriented PET was produced in a two-step-stretching process: the first, in the travel direction, and the second, in the transverse direction. Two biaxially oriented films were studied:

- A PET film (16 μm thick) annealed at 180 °C after the biaxial orientation, denoted as annealed oriented PET and labeled as PETs, allowing a crystallinity stabilization of the film, which process is known as heat-setting;
- A PET film (23 μm thick) unannealed after orientation, denoted as unannealed oriented PET and labeled as PET.

The initial unoriented amorphous PET film was also studied as reference material.

Adhesive tape is constituted by a halogen-free thermoplastic polyester adhesive (23 μm thick) spread out over oriented PET film unannealed (23 μm thick).

The storage effects on adhesive tape were studied over various storage durations ranging from 4 h to several months at room temperature and at 50% RH.

Methods

DSC

DSC measurements were carried out with a TA instrument (2920 CE), using aluminum non-hermetically sealed pans.

Thermograms were recorded at a heating rate of 5 or 10 °C min^{-1}, under a dry helium gas purge at a flow rate of 110 mL min^{-1}. High purity indium and mercury were used for temperature and enthalpy calibration.

The glass transition is defined as the onset of the heat capacity increment. The melting and the crystallization transition temperatures were determined as the temperature of the endothermic peak maximum and the temperature of the exothermic peak minimum, respectively.

We evaluated the degree of crystallinity of PET film, using Eq. 1:

$$\chi_c = \Delta H_{f,net}/\Delta H^0 \quad (1)$$

where ΔH^0 is the heat of fusion of an ideal 100% crystalline, and $\Delta H_{f,net} = \Delta H_f - \Delta H_c$ is the net heat of fusion with ΔH_f being the heat of fusion, and ΔH_c being the heat of crystallization. A value of $\Delta H^0 = 140$ J g^{-1} was used [6]. The heat of crystallization ΔH_c was determined in accordance with the baseline method developed by Mathot [7]. Therefore, ΔH_c value takes into account the slight exothermic effect on recrystallization until the melting point.

DDS

Measurements were carried out with a Novocontrol Broadband Dielectric Spectrometer (BDS4000). The sample was placed into a cryostat between gold-plated stainless steel electrodes of a parallel capacitor. The temperature was controlled with a stability of ±0.01 °C by a cold nitrogen gas stream that was heated by a Quatro temperature controller.

In order to determine the molecular mobility, the measurements of the complex dielectric permittivity

$$\varepsilon^*(F) = \varepsilon'(F) - i\varepsilon''(F) \quad (2)$$

were carried out in the frequency (F) range from 10^{-2} to 3.10^6 Hz. The experimental limit for the loss factor ε'' was about 10^{-4}. The frequency scans were performed isothermally following a temperature step of 5 °C between −150 and 150 °C.

From each isothermal plot, the relaxation modes were described by the double-stretched Havriliak–Negami function [8]:

$$\varepsilon^*(\omega) = \varepsilon_\infty + \frac{\Delta\varepsilon}{\left[1 + (i\omega\tau_{HN})^{\alpha_{HN}}\right]^{\beta_{HN}}} \quad (3)$$

where τ_{HN} is the relaxation time of the Havriliak–Negami model, and $\omega = 2\pi F$ is the angular frequency. The exponents α_{HN} and β_{HN} characterize the width and the asymmetry of relaxation time distribution, respectively.

Results and discussion

PET film

DSC measurements

DSC measurements shown in Fig. 1 were recorded in the temperature range from 50 to 280 °C for PET films. The variation of the heat flow versus temperature T shows, for unoriented amorphous PET, an onset at 70 °C characteristic of the glass transition ($T_g^{PET} = 70$ °C), and a sharp exothermic peak is then observed at $T_c^{PET} = 126$ °C due to the crystallization of a part of amorphous phase. At higher temperature, an endothermic peak centered on $T_m^{PET} = 255$ °C evidences the melting of the crystalline phase. We determined the degree of crystallinity χ_c <3% according to Eq. 1.

The thermogram of the unannealed oriented PET film (PET) in Fig. 1 shows an onset situated in the vicinity of the glass transition with respect to unoriented amorphous PET. Nevertheless, this onset is now suddenly followed by a rather broad exothermic peak at 88 °C. In the case of the annealed oriented PET film (PETs), the thermogram reveals an almost indiscernible onset characteristic of the glass transition. The glass transition region shown in the inset of the figure seems to be superimposed on a slight exothermic event; so, the glass transition temperature cannot be clearly defined. We note that by comparison with the unoriented amorphous PET, the orientation in PET and PETs films does not modify the melting point observed around 255 °C.

Several studies have shown that the degree of orientation influences the thermal behavior of PET film where the crystallization phenomenon appears shifted to lower temperature as the drawing ratio increases [9, 10]. Moreover, a thermal behavior study, which correlated with structural characteristics such as amorphous orientation determined using wide-angle X-ray diffraction, has been recently performed [11]. These authors established that the cold crystallization temperature decreases linearly to the glass transition with increasing degree of amorphous orientation. In agreement with these previous studies, the exothermic events observed in unannealed (PET) and annealed oriented (PETs) films (Fig. 1) have been ascribed to a crystallization phenomenon at lower temperature than that for the unoriented amorphous PET. The orientation induced during the industrial production of films is responsible for a greater molecular mobility of the oriented amorphous phase which is liberated around the glass transition. In comparison with the PET film, the lowest intensity of the crystallization peak in PETs is in agreement with the better stabilization of crystallinity resulting from the heat-setting performed at 180 °C after the orientation of the film.

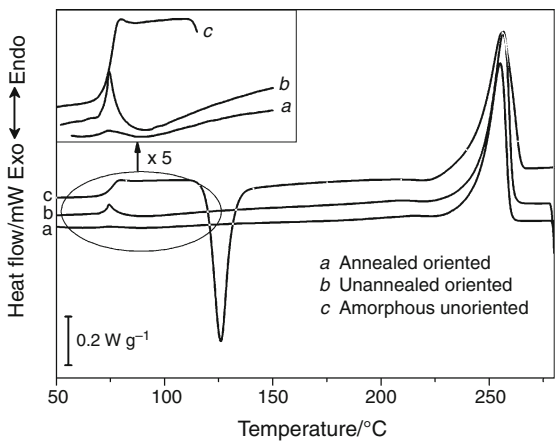

Fig. 1 DSC thermograms obtained with a heating rate of 10 °C min^{-1} on PET films. *a* Annealed oriented, *b* unannealed oriented, and *c* amorphous unoriented

DDS

The recordings of the variation of the dielectric loss ε'' between 10^{-2} and 10^6 Hz, and −150 and 150 °C were performed using DDS measurements on unannealed (PET) and annealed oriented (PETs) films. The dielectric loss surface of unannealed oriented PET film is shown in Fig. 2. These 3D representation reveals at low temperature two broad secondary relaxation modes β^{PET} and β^{PETs}, around the glass transition α_L^{PET} and α_L^{PETs} primary modes, and at higher temperature the α_u^{PET} and α_u^{PETs} modes for unannealed PET and annealed PET films, respectively. The maximum of each mode of relaxation time, τ_{max}, was extracted. Their variations are superimposed in an Arrhenius diagram for unannealed and annealed oriented PET films (Fig. 3). As can be seen, the Arrhenius diagram shows the same behavior of the two secondary relaxation modes. It has been found that the relaxation durations of the β^{PET}, β^{PETs}, α_u^{PET}, and α_u^{PETs} modes are well fitted by an Arrhenius law:

$$\tau(T) = \tau_0 \exp\left(\frac{E_a}{RT}\right) \quad (4)$$

where τ_0 is the pre-exponential factor, E_a the activation energy, R the ideal gas constant.

The α_L^{PET} and α_L^{PETs} modes are ascribed to the dielectric manifestation of the glass transition of the unannealed and annealed oriented PET films, respectively. We note that the two oriented PET films have a sub-mode, denoted as sub-α_L^{PET} in unannealed PET (Fig. 2) and sub-α_L^{PETs} in annealed PET, situated within the glass transition. Nevertheless, each sub-mode hides the α_L^{PET} and α_L^{PETs} modes which are isolated only for the highest frequencies. Therefore, the corresponding τ_{max} values shown in Arrhenius diagram

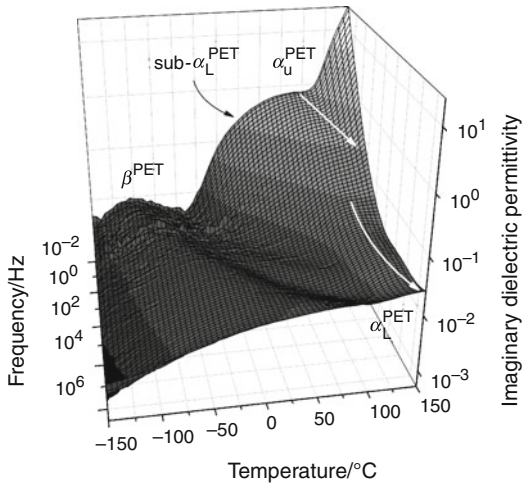

Fig. 2 Dielectric loss surface of unannaled oriented PET film obtained by DDS

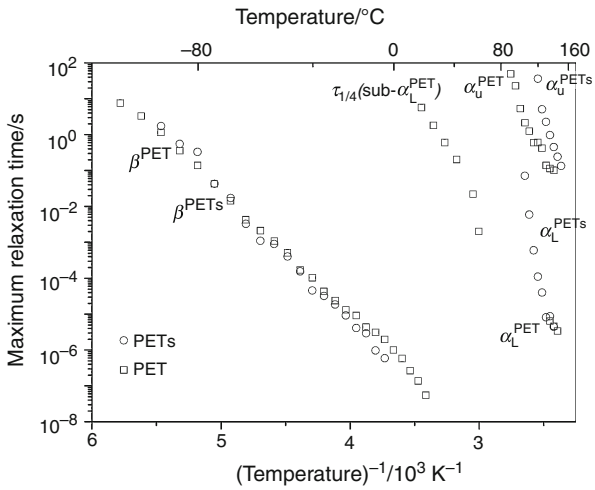

Fig. 3 Arrhenius diagram of relaxation times for oriented PET films obtained by DDS

(Fig. 3) reveal a narrow variation in particular for the unannealed oriented PET film. In the Arrhenius diagram, the τ_{max} variations of both oriented PET and PETs films correspond to same variation. This temperature dependence is not linear in an Arrhenius diagram. It can be described by a Vogel–Tamman–Fulcher (VTF) law:

$$\tau(T) = \tau_{0v}\exp\left(\frac{1}{\alpha_f(T - T_\infty)}\right) \quad (5)$$

where τ_{0v} is a preexponential factor, α_f is the thermal expansion coefficient of the free volume, T_∞ the critical temperature at which any mobility is frozen.

We note that the secondary relaxation mode β^{PET} in Fig. 2 is complex. A similar complex mode β^{PETs} can be observed for the annealed film. Moreover, these two complex modes appear as a broad and asymmetric peak. A previous study on the dynamics involved in this secondary relaxation mode of unoriented amorphous PET, by DDS and thermally stimulated current (TSC) measurements, allowed us to show that this secondary broad mode is constituted of two components β_1 and β_2 [12]. These dielectric techniques give prominence to β_2 process which involves noncooperative mobility of the carbonyl groups motions whereas the relaxation process ascribed to β_1 corresponds to the local motions of the phenyl rings proceeded in a cooperative way.

As seen above, around the glass transition temperature, we make out in Fig. 2 the enhanced molecular mobility for the lowest frequencies between 10^{-2} and 10 Hz ascribed to the sub-α_L^{PET} mode. The same phenomenon is observed for PETs with a sub-α_L^{PETs} mode. We note that this sub-mode is absent in unoriented amorphous PET [13]. These sub-modes appear as a broad shoulder of the α_L^{PET} and α_L^{PETs} primary modes, which does not allow to isolate the corresponding maximum of relaxation time τ_{max}. Therefore, for the unannealed oriented PET film, the area of the sub-mode is evaluated by the variation of $\tau_{1/4}$(sub-α_L^{PET}) determined by the quarter-height of the sub-α_L^{PET} mode, shown as open squares in Fig. 3. This sub-mode situated just below the glass transition seems to traduce a greater molecular mobility resulting from the orientation of amorphous phase. As already observed on the DSC thermogram (Fig. 1), this enhancement of the molecular mobility would be also responsible for the decrease of the crystallization temperature through the glass transition. A sub-α_L mode was already observed in other oriented polymers like PC [14] and PET [10, 15] by TSC and mechanical spectroscopy. This greater molecular mobility is also linked to the increased rate of volume relaxation appearing below T_g^{PET} [14]. Moreover, the electron spin resonance spectroscopy data show that the orientation leads to additional free-volume entities on the small-scale side of the free-volume distribution function [14]. As per this assumption, while the temperature is increasing, just below T_g^{PET}, we observe first that these smallest entities relax, which might explain why the relaxation happens at low temperature. We might even say that the orientation leads to an increased free volume, if we interpret the term "free volume" liberally and use it to mean a measure of segmental mobility and not a simple measure of unoccupied volume [16]. It seems possible that molecular motions responsible for the sub-α_L^{PET} relaxation are associated with some kind of the diffusion process, whereby free volume is distributed into regions of different local density of amorphous phase induced by the orientation [16].

We note that the upper mode corresponding to α_u^{PET} and α_u^{PETs} located above T_g^{PET} was also studied by mechanical means [17] and dielectric techniques where its real nature is often discussed. Up to now, we still do not know the origin of this mode, but its dielectric manifestation can be

related directly (dipolar) or indirectly (ionic) to a motion of macromolecular chains [18].

It was found that the bimodal relaxations, the lower and upper modes situated around and above the glass transition, respectively, are of significant amorphous phase heterogeneity in semicrystalline polymers. Several authors have shown the properties of semicrystalline polymer can be explained by a three-phase model: besides crystalline and mobile amorphous phase (MAP), there is a third phase which has been called oriented [19], anisotropic [20], or rigid amorphous phase (RAP) [21–25]. According to this assumption, these α_L^{PET} and α_L^{PETs} modes are attributed to the MAP responsible for the glass transition observed by DSC measurements, whereas the α_u^{PET} and α_u^{PETs} modes are ascribed to the RAP constrained by crystalline lamellae. Thus, the reduced molecular mobility of RAP is probably due to the existence of more oriented chains than in the case of MAP. The highest temperatures of α_u^{PETs} mode could traduce the strongest constrained chain segments in certain areas of the RAP close to crystallites.

Adhesive tape

DSC measurements

The DSC thermograms shown in Fig. 4 were recorded on adhesive (curves a and b) and adhesive tape (curves c and d), from −40 to 280 °C in both the runs of each sample. The cooling rate here was −20 °C min^{-1}. The first heating runs (curves a and c) performed on as-received samples of adhesive and adhesive tape reveals at low temperature a step of heat flow variation at −27 °C characteristic of the glass transition of the adhesive, denoted as T_{g1}^{adh}. Then, just above the glass transition, these thermograms show a slight exothermic event which appears around $T_{c1}^{adh} = 10$ °C, followed by two small endothermic peaks centered at $T_{m1}^{adh} = 50$ °C and $T_{m2}^{adh} = 125$ °C indicated by arrows on the curves a and c in Fig. 4. Finally, an endothermic peak is only observed at 255 °C on adhesive tape corresponding to the melting point of PET [7]. In the second heating run (curves b and d) performed immediately after cooling from 280 °C, the glass transition temperature of the adhesive increases at $T_{g1}^{*adh} = -15$ °C, and a new small exothermic peak is observed at $T_{c2}^{adh} = 75$ °C, whereas exothermic and endothermic peaks at 10 and 50 °C, respectively, disappear. These transition temperatures are indicated by arrows in Fig. 4. The endothermic peak temperature around $T_{m2}^{adh} = 125$ °C, indicated by arrows, is not modified. Moreover, on the main melting peak of PET at 255 °C appears an additional component characteristic of a new crystalline form of PET due to the thermal conditions imposed during the previous cooling rate.

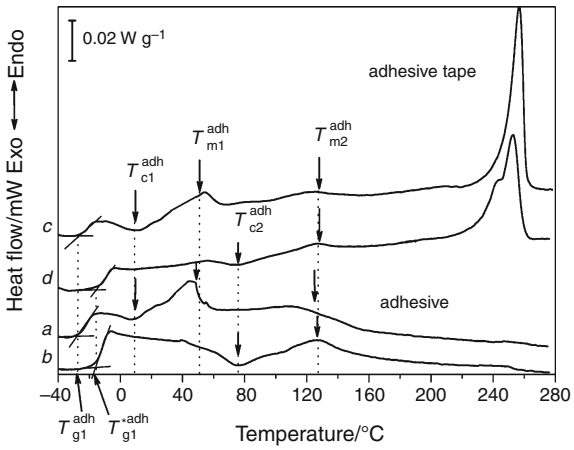

Fig. 4 DSC thermograms of the adhesive *a* 1st heating, *b* 2nd heating and the adhesive tape *c* 1st heating, *d* 2nd heating obtained with a heating rate of 5 °C min^{-1} (*arrows* indicate the position of endothermic peaks and exothermic peaks in each case)

This comparative study gives prominence to similitude of the adhesive and adhesive tape thermograms up to around temperature 180 °C which is situated below the melting region of PET. Therefore, the DSC thermograms, curves a and c in Fig. 4, recorded on as-received samples reveal below 180 °C several transitions attributed to the adhesive: a glass transition T_{g1}^{adh} and one exothermic peak T_{c1}^{adh} characteristic of crystallization which seems to be associated with both melting points T_{m1}^{adh} and T_{m2}^{adh}. We also note that a first heating up to 280 °C performed on as-received adhesive and adhesive tape samples, followed by the subsequent cooling rate of 20 °C min^{-1} result in a reproducible "refreshed" state yielding neither exothermic nor endothermic peak at 20 and 50 °C, respectively, in an immediately following heating run. This "refreshed" state is characterized by a glass transition shifted toward the high temperatures T_{g1}^{*adh}, and a crystallization peak T_{c2}^{adh} associated with the melting peak T_{m2}^{adh}. We also note that the glass transition, the exothermic and endothermic peaks, observed in adhesive alone appears more intense than in the adhesive tape. This evolution traduces that the proportion in mass of adhesive is half in adhesive tape.

Therefore, thermograms of "refreshed" state show the annealing temperature performed above the higher melting point of the adhesive, T_{m2}^{adh}, seems to produce, on the one hand, an evolution of amorphous phase with a significant slight increase of the glass transition temperature T_{g1}^{*adh}, and, on the other hand, a modification of the crystallization kinetic which is traduced by a disappearance of the crystallization and melting points, T_{c1}^{adh} and T_{m1}^{adh}, respectively, but a new crystallization temperature T_{c2}^{adh} appears.

Starting from the reproducible "refreshed" state (Fig. 4, curve d), we hoped to give prominence to the kinetics of the crystalline phase of adhesive by means of various

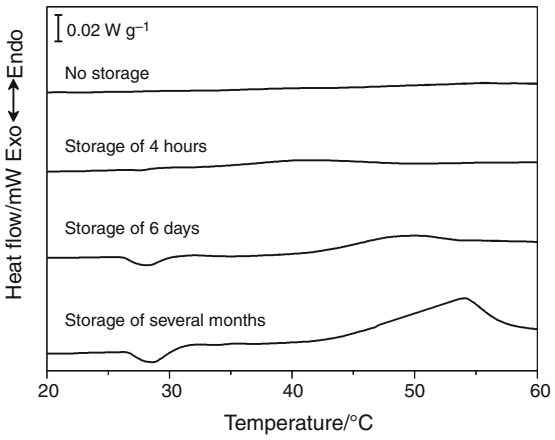

Fig. 5 DSC thermograms of the adhesive tape after storage for various durations, recorded with the heating rate of 5 °C min^{-1} from 20 to 60 °C

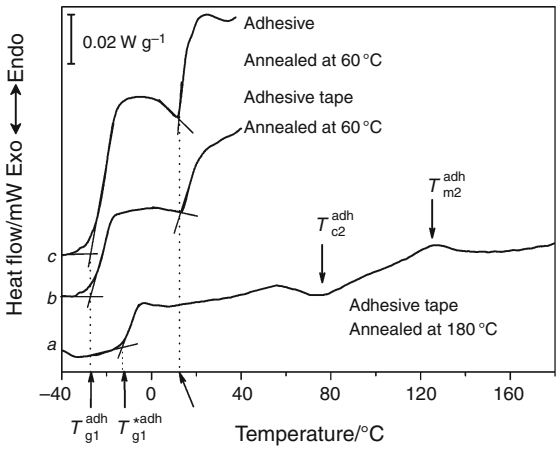

Fig. 6 DSC thermograms of the adhesive tape annealed at 180 °C (*a*) and 60 °C (*b*), and the adhesive annealed at 60 °C (*c*)

storage durations performed on adhesive tape at room temperature (20 °C) prior to the heating run used for detection. Therefore, three relatively short storage durations 4 h, 6 days, and 3 months were performed. In order to get further insight, DSC thermograms obtained on adhesive tape are shown in Fig. 5 in the temperature range from 20 to 60 °C. As the storage duration increases, small exothermic and endothermic peaks appear progressively around 27 and 50 °C, respectively. The manifestation of both peaks upon storage durations is in agreement with the two strongly analogous peaks T_{c1}^{adh} and T_{m1}^{adh} initially observed around the same temperature in the as-received adhesive. Moreover, for each thermogram, the end of its recording at 60 °C is followed by the cooling down of the sample to 20 °C, and an immediate heating allows to record a thermogram labeled no storage in Fig. 5. We note that this thermogram appears as a "refreshed" state in this restricted temperature range. Therefore, this reversible behavior is favorable to associate, on the one hand, with the exothermic peak around 27 °C with the crystallization of a part of adhesive amorphous phase, and, on the other hand, with the endothermic peak at 50 °C with the melting of the corresponding crystalline phase. These experiments provide a direct evidence of crystallization enhancement in adhesive upon storage at room temperature [26]. Therefore, we suppose these storage durations favor formation of poor crystals that reorganize faster on heating at the exothermic peak centered around $T_{c1}^{adh} = 27$ °C, and end up more perfect at the melting temperature around $T_{m1}^{adh} = 50$ °C.

We have verified on the as-received samples that the reproducible "refreshed" state was also obtained after a first heating up to the temperature 180 °C situated just above the highest melting temperature of adhesive T_{m2}^{adh}: an example of DSC thermogram obtained on the adhesive tape submitted to this thermal cycle is shown as curve a in Fig. 6. For this sample, the corresponding values of the temperatures of glass transition $T_{g1}^{*adh} = -15$ °C, crystallization $T_{c2}^{adh} = 75$ °C, and melting $T_{m2}^{adh} = 126$ °C are in agreement with those obtained for the second heating run after annealing at 280 °C (Fig. 4, curve d). Moreover, we observed the slight increase of the glass transition temperature T_{g1}^{*adh} characteristic of amorphous phase evolution on annealing at melting temperature of adhesive T_{m2}^{adh}.

An intermediate annealing process located at a temperature just above of melting point T_{m1}^{adh}, was performed to study the initial structure of amorphous phase of adhesive. Therefore, the evolution of the amorphous phase was minimized by carrying out a first heating up to 60 °C on as-received adhesive and adhesive tape followed by a quenching of the samples to −40 °C. This initial thermal treatment yields neither exothermic nor endothermic peak at 20 and 50 °C on subsequent thermograms recorded on heating run shown in the Fig. 6, curves b and c for adhesive tape and adhesive, respectively. Moreover, these thermograms reveal two glass transitions: the first one T_{g1}^{adh} at −24 °C already observed approximately at the same temperature on as-received adhesive and adhesive tape (Fig. 4, curves a, c), then the second one at $T_{g2}^{adh} = 14$ °C which was not observed in preceding DSC thermograms. We can thus conclude that the first heating run to 60 °C avoids a change in the amorphous phase structure characterized by the glass transition T_{g1}^{adh}, and then the cooling without annealing prevents the crystallization of a part of the amorphous phase. Therefore, these results give prominence to a segregation of two amorphous phases characterized by two glass transitions T_{g1}^{adh} and T_{g2}^{adh}. The heterogeneity of amorphous phase of adhesive could result from a structure constituted of different chain segments to form a blend or a copolymer. As per this proposed assumption, the heating of adhesive until the highest melting temperature T_{m2}^{adh} favors the homogeneity of amorphous phase which is

characterized by only one glass transition temperature T_{g1}^{*adh}. We note that the $T_{g1}^{adh}/T_{m2}^{adh}$ ratio is around 0.63 that is in agreement with the maximum value 0.66 of the distribution ratios obtained for the majority of the polymers [27].

DDS

As the DSC thermograms show, the adhesive influence is observed principally above the room temperature. Therefore, the DDS was studied in the temperature range of the glass transitions observed in the adhesive tape. The 3D variation of the dielectric loss ε'' was recorded by DDS on adhesive tape for temperature range (−30 to 150 °C) and frequency range (10^{-2}–10^{6} Hz). The spectrum obtained reveals the existence of discrete dipolar relaxation modes, and the τ_{max} values extracted from each complex relaxation mode are shown in the Arrhenius diagram (Fig. 7). For comparison, variations of relaxation time obtained on oriented PET films (Fig. 3), unannealed and annealed, are also shown in these Arrhenius diagrams, denoted by open squares and open circles, respectively.

A α_1^{Tape} mode is observed well described by a VTF law (Eq. 5) with parameter values $\alpha_f = 1.15 \times 10^{-3}$ K^{-1}, $\tau_{0v} = 4.9 \times 10^{-13}$ s and $T_\infty = -48$ °C. Its extrapolation at 10^2 s, a characteristic time of the glass transition, agrees with the glass transition temperature of the adhesive, T_{g1}^{adh}, obtained by DSC (Figs. 4, 6). Therefore, the α_1^{Tape} mode is associated with the dielectric manifestation of the low component of the glass transition T_{g1}^{adh} of the adhesive.

This Arrhenius diagram reveals a broad variation of relaxation times associated with the α_2^{Tape} well fitted by an Arrhenius law ($E_a = 94$ kJ mole^{-1} and $\tau_0 = 2.1 \times 10^{-16}$ s), and their variations are located in the continuity of the α_m^{Tape} mode which obeys the VTF law ($\alpha_f = 2.3 \times 10^{-3}$ K^{-1}, $\tau_{0v} = 7.7 \times 10^{-7}$ s, and $T_\infty = 46$ °C). Moreover, the variations, the α_m^{Tape} and α_L^{Tape} modes, are situated in the vicinity of the primary relaxation modes, α_L^{PET} and α_L^{PETs} of the oriented PET samples. It is important to note that the extrapolations of α_2^{Tape} and α_L^{Tape} modes at 10^2 s agree with the corresponding temperature values of T_{g2}^{adh} and T_g^{PET}, respectively. Therefore, the α_2^{Tape} and α_L^{Tape} modes are associated with the dielectric manifestation of the glass transitions T_{g2}^{adh} in adhesive and T_g^{PET} in the PET film, respectively. A relation could exist between α_2^{Tape} and α_m^{Tape} characterized by the continuity of their variations observed in the Arrhenius diagram. Furthermore, according to the Havriliak–Negami function (Eq. 3), the relaxation strength values, $\Delta\varepsilon$, extracted from each complex relaxation mode of the α_2^{Tape}, α_L^{Tape} and α_m^{Tape} modes, are shown in Fig. 8. This diagram reveals that as temperature increases, the amplitude of α_L^{Tape} mode decreases, and it disappears before it reaches the α_m^{Tape} mode. Meanwhile, the amplitude of α_2^{Tape} mode keeps on increasing until it reaches the α_m^{Tape} mode.

This Arrhenius diagram also allows us to remark that the relaxation modes α_{u1}^{Tape} and α_{u2}^{Tape} isolated in adhesive tape coincide with the variations of α_u^{PET} and α_u^{PETs}, respectively. The Arrhenius parameters are as follows: $E_a = 197$ kJ mole^{-1} and $\tau_0 = 5.1 \times 10^{-24}$ s for α_{u1}^{Tape}, and $E_a = 167$ kJ mole^{-1} and $\tau_0 = 9 \times 10^{-21}$ s for α_{u2}^{Tape}.

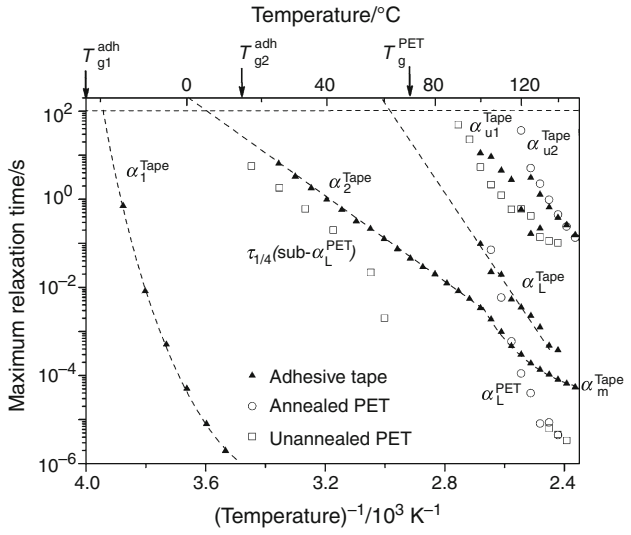

Fig. 7 Arrhenius diagram of relaxation times for adhesive tape, unannealed oriented PET, and annealed oriented PET films obtained by DDS in the temperatures range above −30 °C

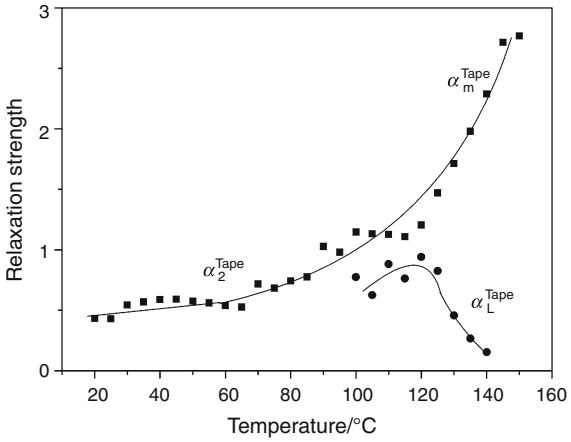

Fig. 8 Temperature dependence of relaxation strength of modes around the glass transition, obtained in adhesive tape

Influence of adhesive on molecular mobility around the glass transition of PET film

Around the glass transition of unannealed oriented PET, the DSC and SDD measurements performed on adhesive tape give prominence to the influence of the adhesive on

the molecular mobility of PET film. In several studies, the mechanical experiments, carried out below and above the glass transition, show that the molecular mobility is responsible for the adhesion between polymer pairs like polystyrene/poly(phenylene oxide) (PS/PPO) [28], PS/PS [2], PET/PET, and PS/PET [29] resulting from the interpenetration of chain segments across the interface. Moreover, in this temperature range, shear strength measurements give prominence on contact time of polymer pair to a one-fourth power law ($t^{1/4}$) which is characteristic of a controlled process by diffusion [29].

As seen before, the SDD spectrum of unannealed oriented PET films (Fig. 2) reveals a sub-α_L^{PET} mode situated below the glass transition. This greater molecular mobility results from the orientation of amorphous phase which is also responsible for the decrease of the temperature of the crystallization through the glass transition observed on DSC thermogram (Fig. 1). It is important to note that this sharp exothermic peak is not observed any more when the adhesive is in contact with film of unannealed oriented PET in adhesive tape (Fig. 4, curve c). Indeed, for temperature around and below the glass transition of the PET, the amorphous phase of the adhesive is in the liquid-like state because it is situated above its second glass transition T_{g2}^{adh} (Fig. 6). Hence, the proposed assumption is that as the temperature increases through the PET glass transition, the mobility of the adhesive chain segments is sufficient to diffuse in the PET disordered structure. The segments of the adhesive cause a steric obstruction in the PET amorphous phase to prevent at T_g^{PET} the abrupt regular arrangement of the chain segments to constitute the crystalline phase. Nevertheless, we note the heat of fusion obtained in the adhesive tape $\Delta H_f = 48$ J g^{-1} (Fig. 4, curve c) is the same value as that calculated from the unannealed oriented PET (Fig. 1). This result traduces a regular slow and progressive crystallization process in adhesive tape during its heating up to the melting temperature equivalent to the sharp crystallization peak obtained in unannealed oriented PET.

The α_m^{Tape} and α_L^{Tape} modes situated in the vicinity of the primary relaxation modes of oriented PET samples could be also characteristic of the diffusion of adhesive polymer molecules into the network of the unannealed oriented PET film. In order to check this hypothesis, the DSC thermogram and the DDS measurements were recorded on the PET film after having removed the adhesive from the adhesive tape which were never heated. The transition spectrum and the dielectric relaxation spectrum obtained were identical to the unannealed oriented PET having never been in contact with the adhesive corresponding to Figs. 1 and 2, respectively. These results confirm that the diffusion of polymer molecules of adhesive into the amorphous phase of the PET film during the heating run is quite responsible for the evolution of the dielectric relaxation modes and transition observed around the glass transition. We note the lower activation energy of α_L^{Tape} modes (168 kJ mol^{-1}) than that of α_L^{PET} (355 kJ mol^{-1}). This weak activation energy is characteristic of the plasticizing effect on relaxation process around the glass transition due to the diffusion of the adhesive chain segments into the PET amorphous phase.

The α_2^{Tape} mode fitted by an Arrhenius law characterized by a weak enthalpy is associated with a weak size distribution of the relaxing species through the glass transition of the adhesive. In the continuity of α_2^{Tape}, the dynamic dielectric technique allows us to show that the α_m^{Tape} mode obeys a new dielectric relaxation behavior corresponding to the VTF law. Therefore, this mode involves the mobility of sequences of the main chain in modified constraining environments. The diffusion of the molecular chain segments of adhesive in PET amorphous phase could be responsible for this behavior evolution. It is interesting to note that the dielectric spectroscopy reveals on adhesive tape two primary relaxation modes, α_m^{Tape} and α_L^{Tape}, which replace α_L^{PET} observed in oriented unannealed PET film. These two primary modes in adhesive tape seem to be due to the influence of the adhesive chain segments on the molecular mobility of the PET amorphous phase. Therefore, as per these assumptions, these two modes are characteristic of amorphous phase heterogeneity in the glass transition region. This heterogeneity could traduce the presence of the interphase between adhesive and PET film.

Conclusions

The combination of the DSC and the DDS has allowed us to explore the transitions and the molecular mobility of an oriented PET film pre-impregnated with a polyester thermoplastic adhesive. The comparative study of this adhesive tape with each component the polyester adhesive and the oriented PET film reveals the influence of the adhesive chain segments on the molecular mobility around the glass transition of the PET film.

We found very good agreement to explain the evolution of the dielectric relaxation modes by a diffusion of adhesive polymer molecules into the amorphous phase of the PET film. Moreover, the heating run favors the diffusion of the adhesive chain segments which is responsible for the appearance of a wide distribution of dielectric relaxation process in the glass transition region of PET. This distribution is constituted of two modes characterized by an activation enthalpy lower than that of PET alone, due to a plasticizing effect of the adhesive chain. This behavior of the molecular mobility seems to be the result of the heterogeneity of the PET amorphous phase in the adhesive tape.

References

1. Voyutskii SS, Vakula VL. The role of diffusion phenomena in polymer-to-polymer adhesion. J Appl Polym Sci. 1963;7:475–91.
2. Boiko YM, Prud'Homme RE. Surface mobility and diffusion at interfaces of polystyrene in the vicinity of the glass transition. J Polym Sci B Polym Phys. 1998;36:567–72.
3. Baldan A. Adhesively-bonded joints and repairs in metallic alloys, polymers and materials: adhesives, adhesion theories and surface pretreatment. J Mater Sci. 2004;39:1–49.
4. Thomason JL. Investigation of composite interphase using dynamic mechanical analysis: artifacts and reality. Polym Comp. 1990;11:105–13.
5. Garton A, Daly JH. Characterization of the aramid: epoxy and carbon: epoxy interphases. Polym Comp. 1985;6:195–200.
6. Schmidt-Rohr K, Hu W, Zumbulyadis N. Elucidation of the chain conformation in a glassy polyester, PET, by two-dimensional NMR. Science. 1998;280:714–7.
7. Mathot BF. Calorimetry and thermal analysis of polymers. Munich: Hanser Publishers; 1994.
8. Havriliak S, Negami S. A complex plane analysis of α-dispersions in some polymer systems. J Polym Sci C Polym Symp. 1966;14:99–117.
9. Vallat MF, Plazek DJ. Effect of thermally treatment on biaxially oriented poly(ethylene terephthalate). II. The anisotropic glass temperature. J Polym Sci B Polym Phys. 1988;26:545–54.
10. Bernès A, Chatain D, Lacabanne C. Differential scanning calorimetry and thermostimulated current spectroscopy for the study of molecular orientation in polymers. Thermochim Acta. 1992;204:69–77.
11. Bhoje Gowd E, Ramesh C, Byrne MS, Sanjeeva Murthy N, Radhakrishnan J. Effect of molecular orientation on the crystallisation and melting behavior in poly(ethylene terephthalate). Polymer. 2004;45:6707–12.
12. Ménégotto J, Demont P, Bernès A, Lacabanne C. Combined dielectric spectroscopy and thermally stimulated currents studies of the secondary relaxation process in amorphous poly(ethylene terephthalate). J Polym Sci B Polym Phys. 1999;37:3494–503.
13. Ménégotto J, Demont P, Lacabanne C. Study of dielectric relaxation processes of PET by dynamic dielectric and thermostimulated spectroscopies. In: Proceedings of the 10th International Symposium on Electrets (ISE 10). vol. 10; 1999. p. 289–92.
14. Bartos J, Müller J, Wendorff JH. Physical ageing of isotropic and anisotropic polycarbonate. Polymer. 1990;31:1678–84.
15. Dargent E, Santais JJ, Saiter JM, Bayard J, Grenet J. Dielectric relaxations in drawn semi-crystalline poly(ethylene terephthalate). J Non-Cryst Solids. 1994;172–174:1062–5.
16. Song HH, Roe RJ. Structural change accompanying volume change in amorphous polystyrene as studied by small and intermediate angle X-ray scattering. Macromolecules. 1987;20:2723–32.
17. Vigier G, Tatibouet J, Benatmane A, Vassoille R. Amorphous phase evolution during crystallization of poly(ethylene-terephthalate). Colloid Polym Sci. 1992;270:1182–7.
18. Kressmann R, Sessler GM, Günther P. Space-charge electrets. IEEE Trans Dielectr Electr Insul. 1996;3:607–23.
19. Hristov HA, Schultz JM. Thermal response and structure of PET fibers. J Polym Sci B Polym Phys. 1990;28:1647–63.
20. Murthy NS, Correale ST, Minor H. Structure of the amorphous phase in crystallizable polymers: poly(ethylene terephthalate). Macromolecules. 1991;24:1185–9.
21. Menczel J, Wunderlich B. Glass transition of semicrystalline macromolecules. Polymer. 1986;27:255–6.
22. Kattan M, Dargent E, Grenet J. Relaxations in amorphous and semi-crystalline polyesters. J Therm Anal Calorim. 2004;76:379–94.
23. Menczel JD, Jaffe M. How did we find the rigid amorphous phase? J Therm Anal Calorim. 2007;89:357–62.
24. Slobodian P. Rigid amorphous fraction in poly(ethylene terephthalate) determined by dilatometry. J Therm Anal Calorim. 2008;94:545–51.
25. Chen H, Cebe P. Vitrification and devitrification of rigid amorphous fraction of PET during quasi-isothermal cooling and heating. Macromolecules. 2009;42:288–92.
26. Xenopoulos A, Wunderlich B. Thermodynamic properties of liquid and semicrystalline linear aliphatic polyamides. J Polym Sci B Polym Phys. 1990;28:2271–90.
27. Van Krevelen DW. Properties of polymers. Amsterdam: Elsevier; 1972.
28. Boiko YM, Prud'Homme RE. Strength development at the interface of amorphous polymers and their miscible blends, below the glass transition temperature. Macromolecules. 1998;31:6620–6.
29. Boiko YM, Guérin G, Marikhin VA, Prud'Homme RE. Healing of interfaces of amorphous and semi-crystalline poly(ethylene terephthalate) in the vicinity of the glass transition temperature. Polymer. 2001;42:8695–702.